Electronic Supplementary Information

Hybrid Bimetallic-N4 Electrocatalyst Derived from a Pyrolyzed Ferrocene-Co-corrole Complex for Oxygen Reduction Reaction

Satyanarayana Samireddi,[abcd] Indrajit Shown,[a] Tzu-Hsien Shen,[a] Hsin-Chih Huang,[d] Ken-Tsung Wong,[ae] Li-Chyong Chen*[d] and Kuei-Hsien Chen*[ad]

[a]Institute of Atomic and Molecular Sciences, Academia Sinica, Taipei 10617, Taiwan

[b]Molecular Science and Technology, Taiwan International Graduate Program, Academia Sinica, Taipei, Taiwan

[c]Department of Chemistry, National Tsing Hua University, Hsinchu, Taiwan

[d]Center for Condensed Matter Sciences, National Taiwan University, Taipei 10617, Taiwan

[e]Department of Chemistry, National Taiwan University, Taipei 10617, Taiwan

*Email - chenkh@pub.iams.sinica.edu.tw, chenkh168@gmail.com

Experimental Section

Materials: All commercially available chemical reagents and solvents (Sigma-Aldrich, Merck and Acros) were of synthetic grade and used without any further purification. Silica gel 60 (70–230 mesh), neutral alumina and basic alumina (Brockmann grade III) obtained from Merck were used for column chromatography and silica gel coated plates were used for thin layer chromatography. A 2.5 cm diameter of column was used to perform all the column chromatographic experiments. The column running time was varied according to the requirement by the application of different pressures from the top of the column, which is an important factor for obtaining final FCC product.

***Instrumentation*:** ^{1}H and ^{13}C NMR spectra were recorded in $CDCl_3$ at 300 K with a Bruker Advance (400 MHz) spectrometer and all the data was processed with TopSpin. Chemical shifts are given in ppm relative to a residual solvent (7.26 ppm for ^{1}H and 77.3 ppm for ^{13}C). A FINNIGAN MAT 95S Mass Spectrometry instrument operating in ESI mode was used to get the high resolution mass spectra. UV-Vis spectra were measured in DCM with Jasco V-670 spectrophotometer using a 10 mm quartz cell. FT-IR spectra were measured using Thermo Nicolet 6700 spectrometer by ATR mode. The content of C and N was collected by an elemental analyzer of Elementar vario EL cube, while the metal content (Fe and Co) was obtained by ICP-MS of Perkin Elmer, SCIEX ELAN 5000. SEM (filed emission, JEOL, JSM-6700F) and TEM (JEOL JEM-2100) were used to see the morphology and elemental mapping. Powder XRD was carried out using a Bruker D2 phaser diffractometer system with Cu Kα1 radiation ($\lambda = 1.54056$ Å). The TGA measurement was carried out using a TGA Q500 V20.13 Build 39 instrument at a scanning rate of 5 °C min^{-1} from room temperature up to 800 °C , while the sample was kept in a constant

flow of N_2 gas. Raman spectrum of the samples was measured using a Jobin-Yvon LabRAM HR800-Confocal micro-Raman spectroscope with a 633 nm He–Ne laser as the excitation source. The XPS (VG ESCA Scientificc Theta Probe) data was recorded using 1486.6 eV Al Kα source. All the binding energies were calibrated with the graphitic C (1s) core level value of 284.5 eV. Moreover, all the peaks were deconvoluted using SDP software (version 4.1) with 90% Gaussian−10% Lorentzian peak fitting.

Single crystal X-ray crystallographic data collection of FCC was carried out on a BRUKER SMART APEX CCD diffractometer with Mo radiation (λ = 0.71073 Å) at 150(2) K. After data collection, the frames were integrated and absorption corrections were applied. Using SHELXTL program on PC computer made the structure analysis. The structure was solved using the SHELXS-97 program and refined using SHELXL-97 program by full-matrix least squares on F2 values.[1] All of the non-hydrogen atoms are refined anisotropically. Hydrogen atoms attached to the carbons were fixed at calculated positions and refined using a riding mode. Drawings were produced using Diamond 3.0 software. These data is obtained free of charge from The Cambridge Crystallographic Data Centre via www.ccdc.cam.ac.uk/data_request/cif.

***Synthesis of 10-ferrocenyl-5,15-diphenyl corrole (1)*:** Ferrocenecarboxaldehyde (1.0 g, 4.6 mmol) and 5-phenyldipyrromethane (2.1 g, 9.5 mmol) were dissolved in 300 ml methanol, and then 300 ml of 0.6 M HCl was slowly added to the above solution after which the reaction was maintained at room temperature for 2- 3 hours. Further, the reaction mixture (RM) was extracted with chloroform followed by two times organic layer washings with water after which organic phase was dried over $MgSO_4$ and diluted to 600 ml. To this reaction mixture, DDQ was added and maintained the reaction for 1-2 hours. Then the RM was filtered on a celite bed and the solvent was removed under reduced pressure. Finally, the crude using hexane: DCM (1:1) mixture was

filtered through silica packed short column and the compound (1) was obtained after removing the solvent. Yield = 14.2% (0.42 g).

***Synthesis of FCC (2)*:** 10-ferrocenyl-5, 15-diphenyl corrole (0.42 g, 0.66 mmol) was dissolved in minimum amount of DCM (normally less than 10 ml) and then diluted with 500 ml ethanol after which $CH_3COONa.3H_2O$ (0.45 g, 3.3 mmol) followed by $Co(CH_3COOH)_2.4H_2O$ (0.74 g, 2.3 mmol) and PPh_3 (0.24 g, 0.92 mmol) were added. The RM was slowly turned to reddish brown color and further the reaction was maintained for 12-15 hours at room temperature. Thereafter, the RM was extracted with DCM and further the DCM layer was washed few times with water till the ethanol was completely recovered into water. Then short silica packed filtration was done quickly after which the obtained crude was used for column chromatography. The final optimized column chromatography parameters were; eluent (DCM: Hexane = 60:40), column packing length was 12 cm with diameter of 2.5 cm and the column running time should not be more than 10 min. Yield: 68 mg, 1.5% (starting from ferrocenecarboxaldehyde). ^{1}H NMR (400 MHz, $CDCl_3$, 25 ºC): δ (ppm) 9.2 (d, J = 5.2 Hz, 2H; β-pyrrole), 8.5 (d, J = 3.6 Hz, 2H; β-pyrrole), 8.3 (d, J = 5.2 Hz, 2H; β-pyrrole), 8.1 (br, H), 8.0 (d, J = 4.4 Hz, 2H; β-pyrrole), 7.7 (m, 2H; 4-ring-Ph), 7.6 (br, 4H; 2-ring-Ph), 7.5-7.4 (m, 4H; 3-ring-Ph), 7.08-7.04 (m, 3H; 4-PPh_3), 6.77-6.73 (m, 6H; 3-PPh_3), 5.24 (t, J = 2x1.6, 2H; 2′-Fc), 4.81-4.76 (m, 6H; 2-PPh_3), 4.62 (t, J = 2x1.6, 2H; 3′-Fc), 4.1 (s, 5H; 4′-Fc), 5.3 (s, DCM solvent peak).[2] ^{13}C NMR (400 MHz, $CDCl_3$, 25 ºC): δ (ppm) 146.2 (C-9, C-11), 144.3 (C-6, C-14), 142.0 (C-4, C-16), 136.5 (C-1, C-19), 132.3 (C-7, C-13), 131.8 (C-8, C-12), 131.7 (C-3, C-17), 131.5 (C-2, C-18), 130.8 (C1, ring-Ph)[a], 129.2 (C4, ring-Ph)[a], 128.5 (C2, ring-Ph) [a], 127.7 (C3, ring-Ph)[a], 127.0 (C1, PPh_3)[b], 125.9 (C4, PPh_3)[b], 125.0 (C2, PPh_3)[b], 124.6 (C3, PPh_3)[b], 123.8 (C-5, C-15), 118.6 (C-10), 90.9 (1′-Fc), 73.4 (3′-Fc), 70.1 (4′-Fc), 67.9 (2′-Fc), 53.4

(DCM solvent peak).[2] HRMS-ESI *m/z*: $[M + H]^+$ calcd. for $C_{59}H_{43}N_4PCoFe$, 953.1901; found, 953.1938. [a,b]Signal assignment may be exchanged, Fc: Ferrocene.

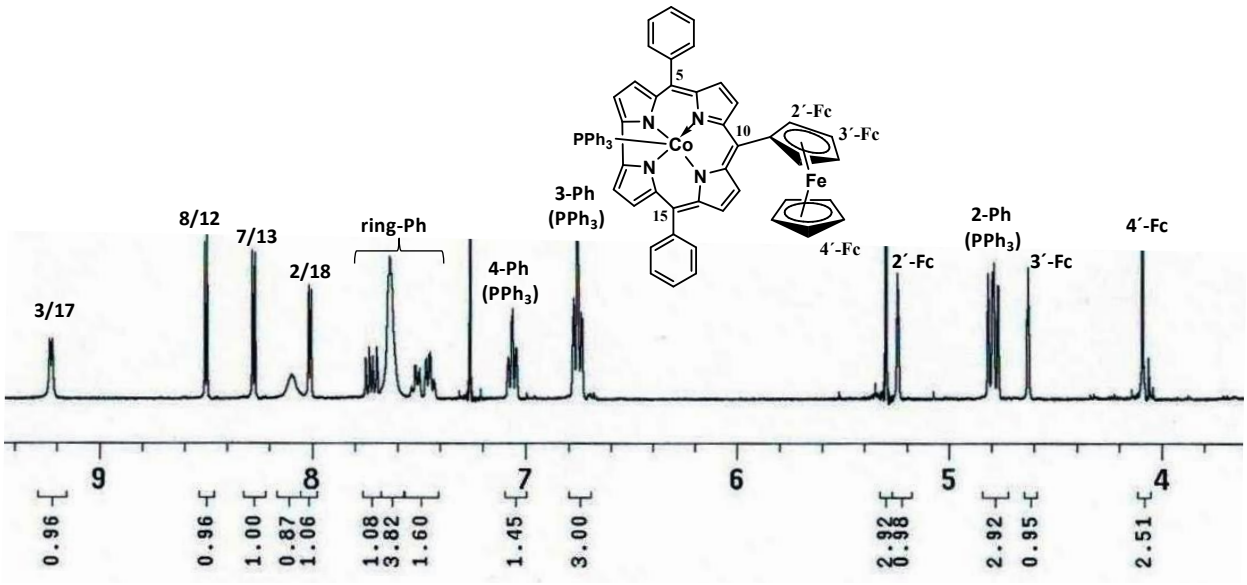

Fig. S1 ^{1}H NMR spectra of FCC in $CDCl_3$.

Table S1 Crystal data and structure refinement of FCC.

Empirical formula	C60 H42 Co Fe N4 O P	
Formula weight	980.73	
Temperature	150(2) K	
Wavelength	1.54178 Å	
Crystal system	Orthorhombic	
Space group	Fdd2	
Unit cell dimensions	a = 24.7816(4) Å	α= 90°.
	b = 47.5380(8) Å	β= 90°.
	c = 15.4054(3) Å	γ = 90°.
Volume	18148.6(6) $Å^3$	
Z	16	
Density (calculated)	1.436 Mg/m^3	
Absorption coefficient	6.145 mm^{-1}	
F(000)	8096	
Crystal size	0.15 x 0.10 x 0.10 mm^3	
Theta range for data collection	3.50 to 67.99°.	
Index ranges	-27<=h<=29, -40<=k<=56, -13<=l<=18	
Reflections collected	10196	
Independent reflections	5958 [R(int) = 0.0448]	
Completeness to theta = 67.99°	99.1 %	
Absorption correction	Semi-empirical from equivalents	
Max. and min. transmission	1.00000 and 0.74346	
Refinement method	Full-matrix least-squares on F^2	
Data / restraints / parameters	5958 / 3 / 624	
Goodness-of-fit on F^2	1.024	
Final R indices [I>2sigma(I)]	R1 = 0.0551, wR2 = 0.1407	
R indices (all data)	R1 = 0.0634, wR2 = 0.1483	
Absolute structure parameter	-0.014(5)	
Largest diff. peak and hole	1.267 and -0.523 e.$Å^{-3}$	

Table S2 Selective bond distances (Å), bond angles (°) and Torsion angles (°) of FCC

Bond distances (Å)		bond angles (°)		Torsion angles (°)	
Co(1)-N(1)	1.869(5)	N(1)-Co(1)-N(4)	80.9(2)	C9 C10 C32 C36	-51.4(8)
Co(1)-N(4)	1.877(5)	N(1)-Co(1)-N(2)	89.9(2)	C11 C10 C32 C33	-45.1(8)
Co(1)-N(2)	1.882(5)	N(4)-Co(1)-N(3)	89.6(2)	C4 C5 C26 C27	-56.5(1)
Co(1)-N(3)	1.892(4)	N(2)-Co(1)-N(3)	94.3(2)	C6 C5 C26 C31	-58.3(9)
Co(1)-P(1)	2.205(17)	N(4)-Co(1)-N(2)	161.5(2)	C14 C15 C20 C21	72.9(8)
		N(1)-Co(1)-N(3)	161.0(2)	C16 C15 C20 C25	66.0(9)
		N(1)-Co(1)-P(1)	101.03(15)		
		N(4)-Co(1)-P(1)	97.55(16)		
		N(2)-Co(1)-P(1)	100.00(15)		
		N(3)-Co(1)-P(1)	96.50(15)		

***Electrochemical Measurements*:** All electrochemical reactions were conducted in a three-electrode cell using a potentiostat/galvanostat instrument (Biologic Bi-stat). The working electrode used during experiments was the RRDE (PINE AFE6R2GCPT) made of a GC disk and a platinum ring. The reference electrode used was a saturated calomel electrode (0.242 V vs. NHE), while the counter electrode was a Pt wire. All the potentials, here, in this work are mentioned with reference to the RHE. Always an oxygen-saturated 0.1 M $HClO_4$ solution was used as an electrolyte during the ORR measurements.

The Oxygen reduction during electrochemical measurement follows mainly in the following pathways,

$O_2 + 4H^+ + 4e^- \rightarrow 2H_2O$ $E^0 = 1.229$ V ——1—

$O_2 + 2H^+ + 2e^- \rightarrow H_2O_2$ $E^0 = 0.695$ V ——— 2

$H_2O_2 + 2H^+ + 2e^- \rightarrow 2H_2O$ $E^0 = 1.763$ V ——— 3

The cathode catalytic part in the fuel cell device is damaged due to the killing effect of H_2O_2 formation when the ORR follows the above second reaction pathway, therefore the catalyst which follows the four electron pathways is always preferred than two electron. From the RRDE method during ORR, the electron transfer number (n) and $\%H_2O_2$ are calculated according to the following equations:

$$n = \frac{4\ |id|}{|id| + |ir|/N}$$

$$\%\ H2O2 = \frac{2\ |ir|/N}{|id| + |ir|/N} \times 100$$

where i_d is the disk current, i_r is the ring current and N is the collection efficiency (N=38.3%). On the other hand, the electron transfer number can also be estimated by rotating disk electrode (RDE) method using Koutecky–Levich (K-L) equation,

$$\frac{1}{j} = \frac{1}{j_K} + \frac{1}{j_D} = \frac{1}{j_K} + \frac{1}{B\omega^{1/2}}$$

where, $B = 0.62nFACD^{2/3}v^{-1/6}$

In the above equation, j is the experimental current, j_K is the kinetic current, j_D is the diffusion-limiting current, ω is the angular velocity of the disk, n is the electron transfer number, F is Faraday's constant (96485 C/mol), A is the geometric area of RDE electrode (0.237 cm^2), C is the dissolved oxygen concentration in 0.1 M $HClO_4$ electrolyte (1.26 x 10^{-3} mol/lit), D is the diffusion coefficient of oxygen in 0.1 M $HClO_4$ (1.93 x 10^{-5} cm^2/s) and υ is the viscosity of the

electrolyte (0.01 cm^2/s).[3] At various potentials, the graph between 1/j vs. $1/\omega^{1/2}$ ($\omega=2\pi N$, N is the linear rotation speed) gives the slope from which the n values can be calculated according to the K-L equation.

For measuring active surface area of the catalyst, the C_{dl} is estimated to be linearly proportional to the effective ESA of the electrode.[4] The accurate ESA calculation is difficult to measure due to the unknown capacitive behavior of the Py-FCC/C catalysts; however the relative ESA can be estimated by C_{dl} values by employing simple CV method. Since there was no observation of faradic currents between the potential ranges of 0.01-0.21 V vs. RHE, the different lower values of scan rates for measuring the capacitance were employed (Fig. S4). Further, the capacitive currents of $|j_a-j_c|_{0.11V \text{ vs. RHE}}/2$ were plotted as a function of CV scan rate ranges from 1-20 mV s^{-1} (Fig. 3b). The obtained data were fitted to a linear regression, from which the slope calculated is the geometric C_{dl}.[5]

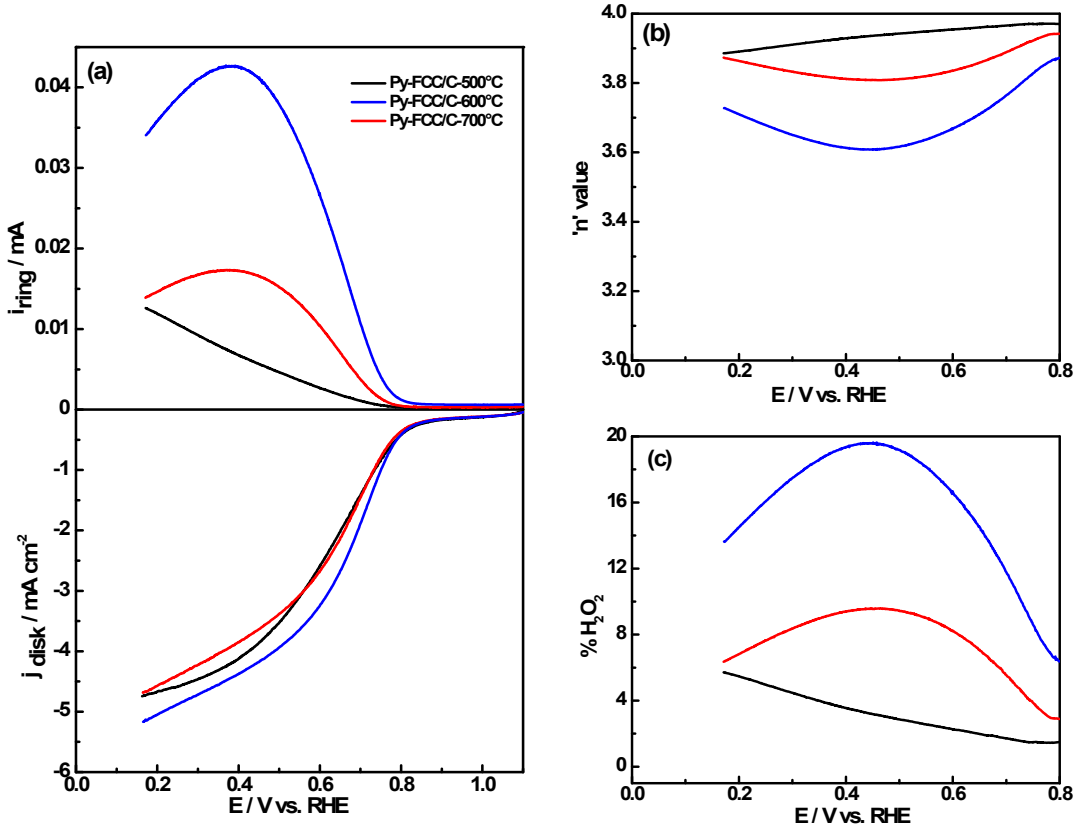

Fig. S2 LSV curves of pyrolyzed FCC/C catalyst obtained at 500, 600 and 700 °C (a) disk currents (below) and ring currents (above), (b) electron transfer number and (c) $\%H_2O_2$ yield. (electrolyte: O_2-saturated 0.1 M $HClO_4$, sweep rate: 10 mV s^{-1}, electrode rotation speed: 1600 rpm, counter electrode: Pt wire).

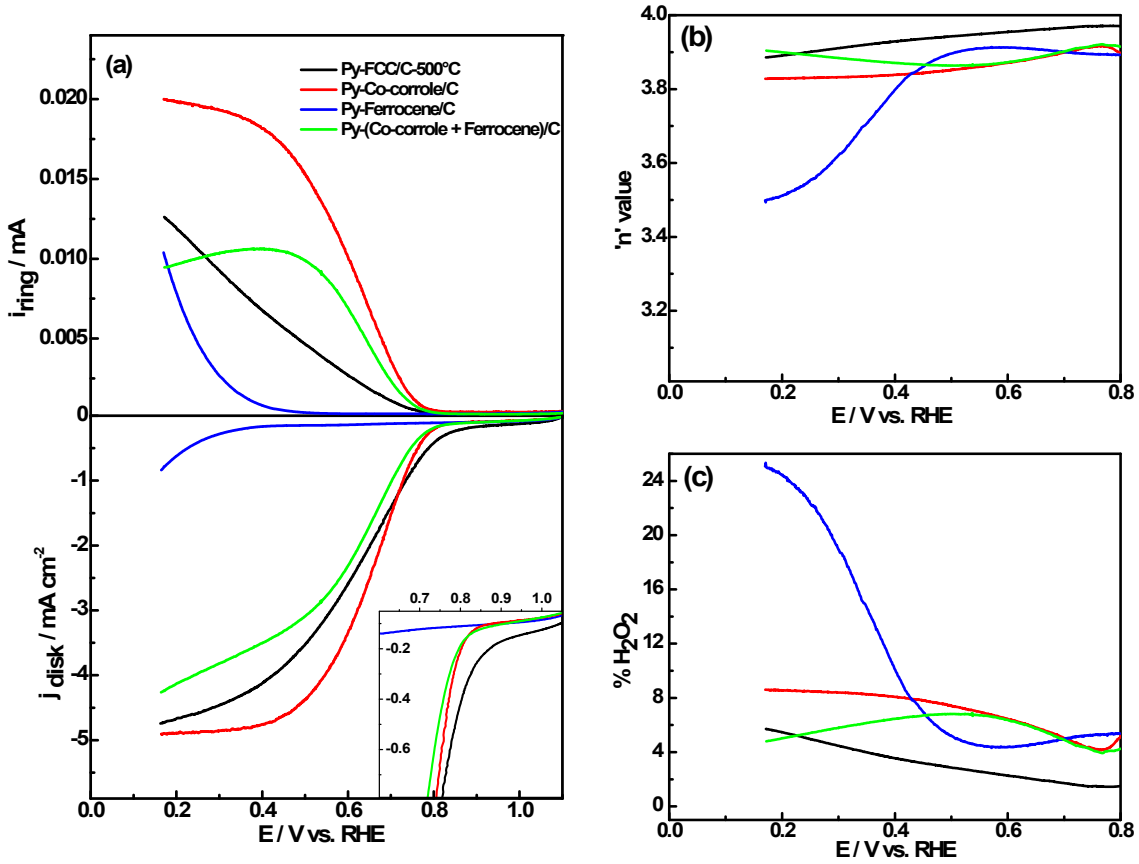

Fig. S3 LSV curves of Py-FCC/C-500°C, Py-Co-corrole/C, Py-Ferrocene/C and Py-(Co-corrole + Ferrocene)/C in O_2-saturated 0.1 M $HClO_4$ (a) disk currents (below), its enlarged onset region (inset) and ring currents (above) (b) electron transfer number and (c) $\%H_2O_2$ yield. (sweep rate: 10 mV s^{-1}, electrode rotation speed: 1600 rpm, counter electrode: Pt wire).

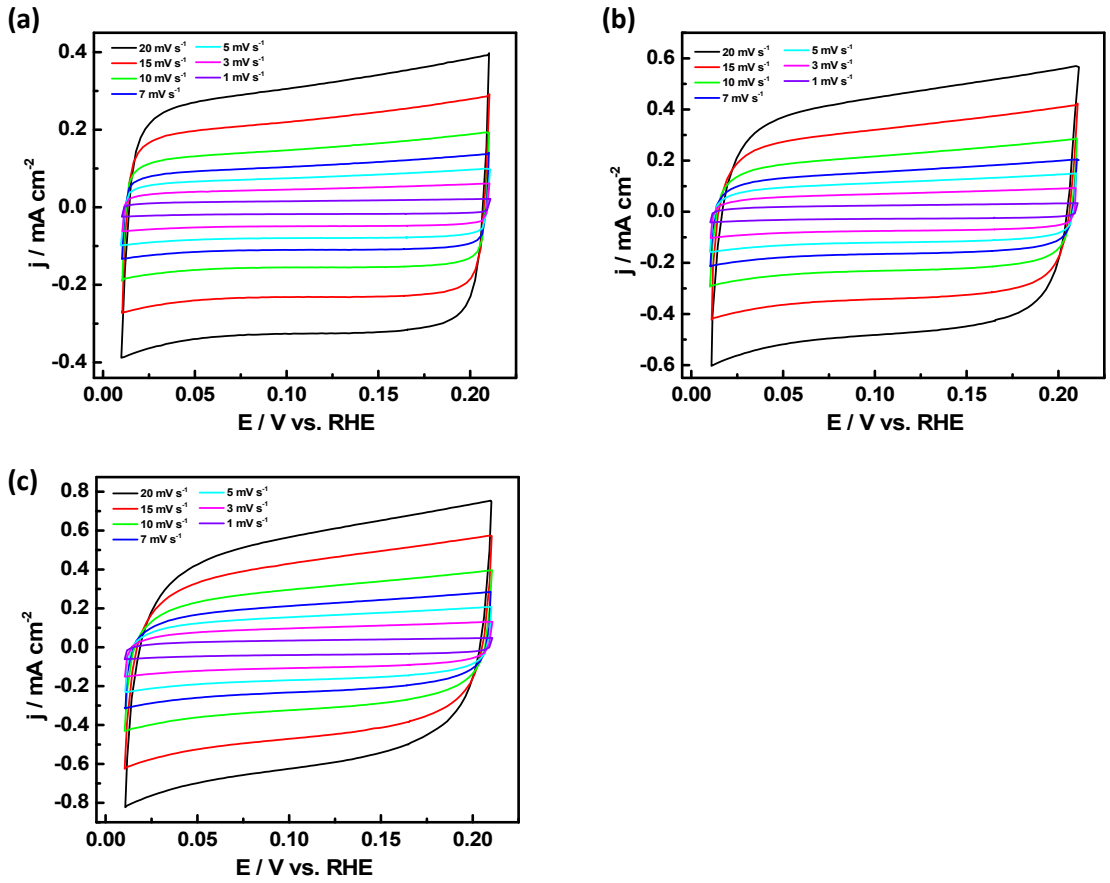

Fig. S4 CV curves of (a) Py-FCC/C-20, (b) Py-FCC/C-33 and (c) Py-FCC/C-50 in the region of 0.01V-0.21V vs. RHE.

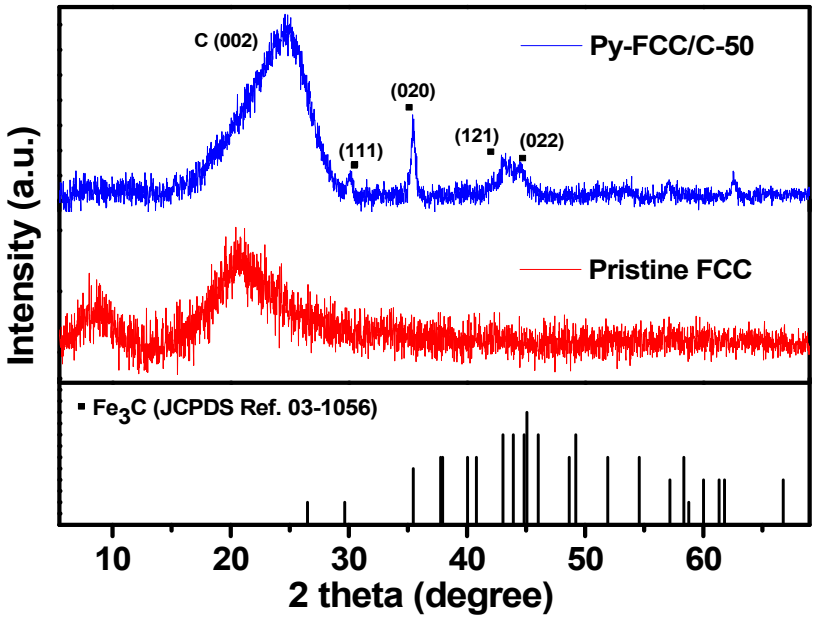

Fig. S5 Powder XRD patterns of pristine FCC and Py-FCC/C-50.

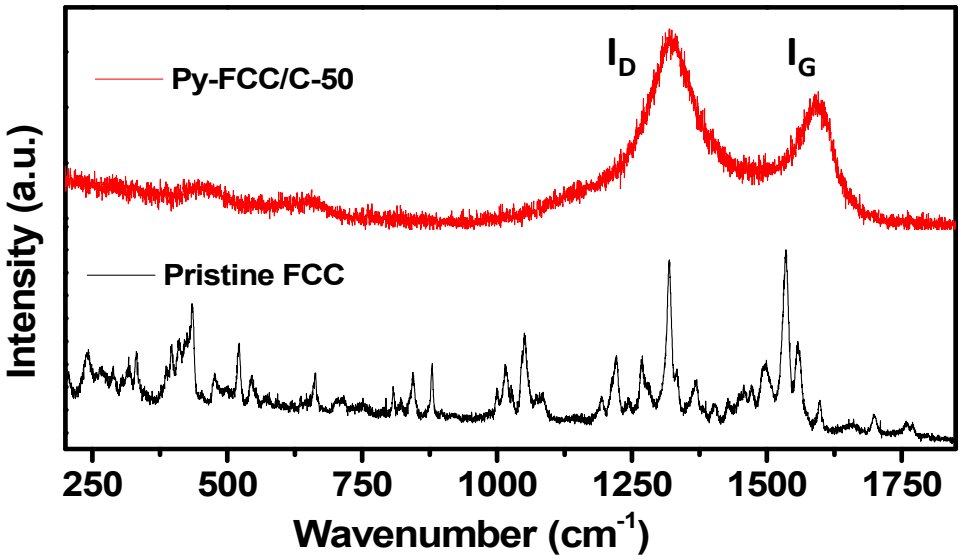

Fig. S6 Raman spectra of pristine FCC and Py-FCC/C-50.

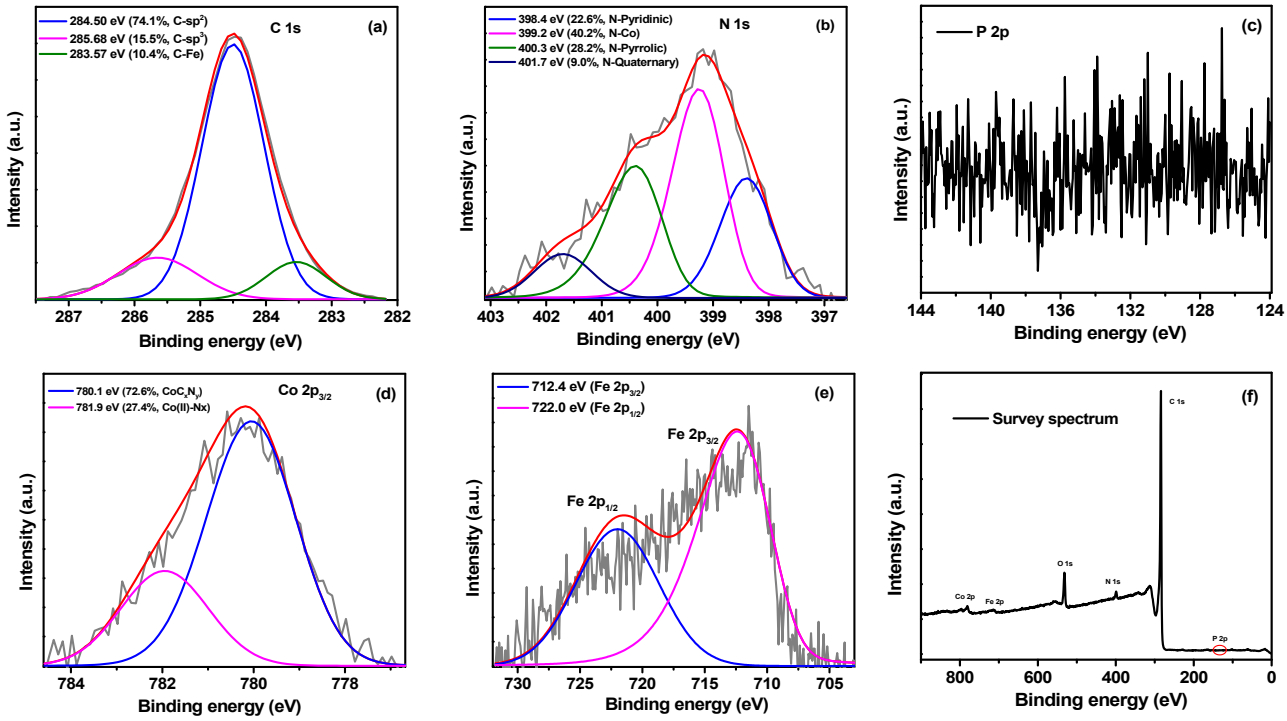

Fig. S7 XPS spectra of Py-FCC/C-50; (a) C 1s, (b) N 1s, (c) P 2p, (d) Co 2p, (e) Fe 2p and (f) survey spectrum

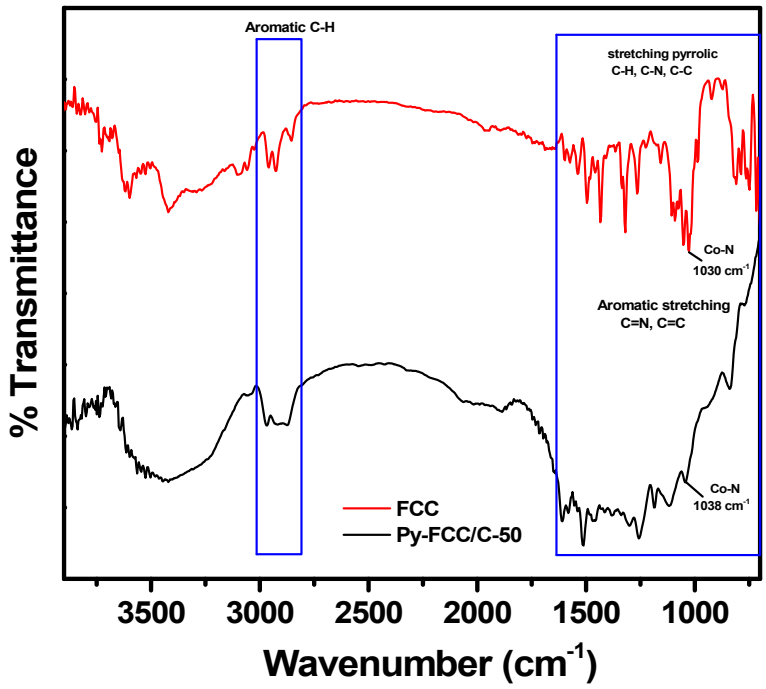

Fig. S8 FT-IR comparison spectra of precursor FCC and its pyrolyzed Py-FCC/C-50 catalyst.

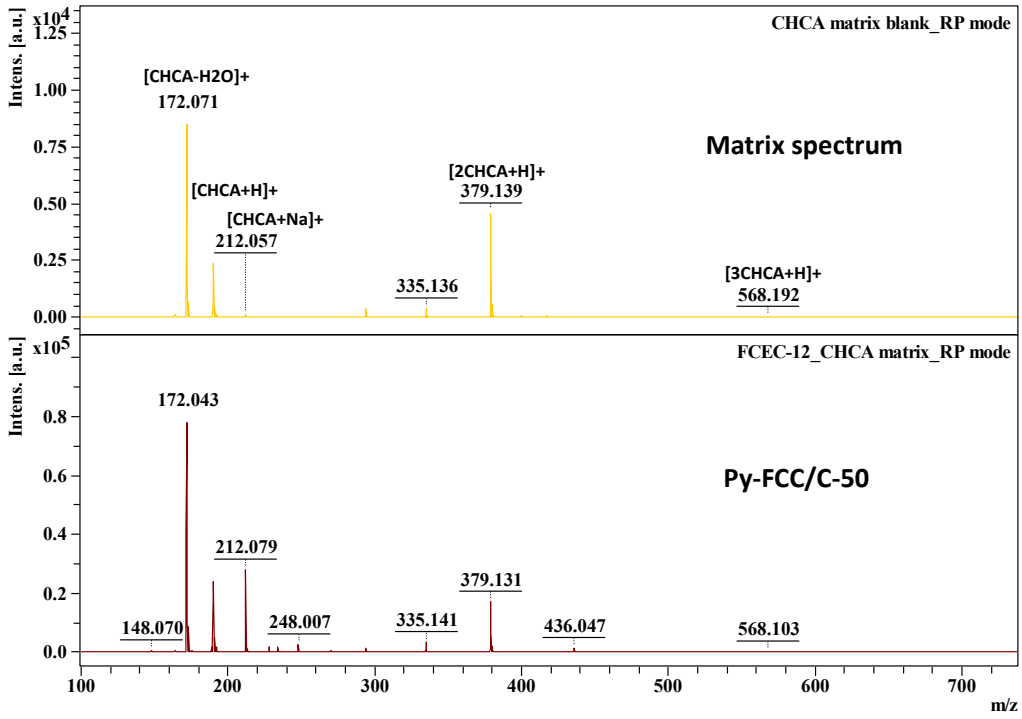

Fig. S9 Comparison spectrum of Py-FCC/C-50 with MALDI matrix, obtained from MALDI mass analysis.

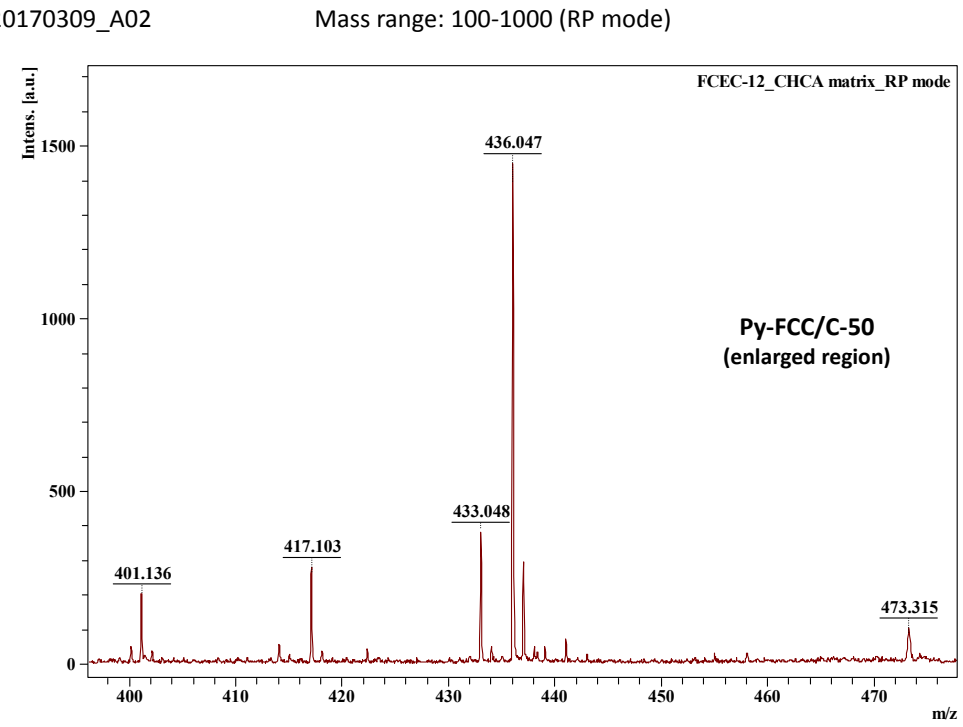

Fig. S10 Enlarged spectrum of Py-FCC/C-50 obtained from MALDI mass analysis.

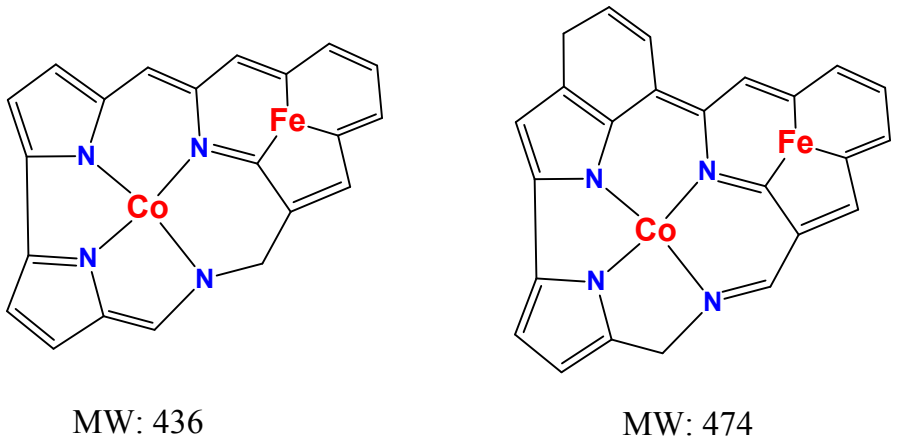

MW: 436 MW: 474

Fig. S11 Possible mass fragmented products , according to MALDI mass spectra of Py-FCC/C-50 as represented in Fig. S9 and 10.

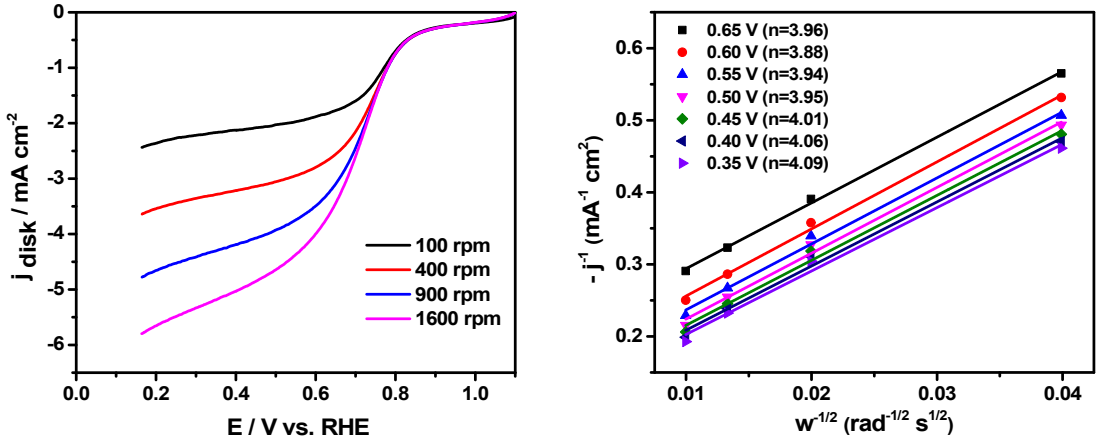

Fig. S12 (a) ORR polarization curves of Py-FCC/C-50 at different rotation speeds in O_2-saturated 0.1 M $HClO_4$ with a sweep rate of 10 mV s^{-1} using Pt-wire counter electrode and the corresponding (b) linear fitting K-L plots at various potentials.

Table S3 The n values and $\%H_2O_2$ yilelds of Py-FCC/C-50, Py-Co-corrole/C-50 and 20% Pt/C calculated from the corresponding disk and ring currents in the potential range of 0.2 to 0.8 V.

	20% Pt/C	Py-FCC/C-50	Py-Co-corrole/C-50
Electron transfer number (n)	3.97-3.99	3.95-3.98	3.84-3.92
% H_2O_2 yield	0.7-1.2	0.7-2.3	3.6-7.8

Table S4 A comparsion of the non-precious electrocatalysts containing Co and/or Fe with N-containing carbons for ORR in acidic medium

Catalyst name	Catalyst property				Comparasion with Pt/C		Ref.
	$E_{1/2}$	onset	n	$\%H_2O_2$ yield	$E_{1/2}$	onset	
Fe-ODAN-1%	0.75	0.8	~ 4.0	below 4%	0.81	0.87	6
FeCo-N/C	~ 0.68	~78	3.88	below 10%	-	-	7
ZIF-67-900-AL	~ 0.76	0.85	3.8-4.0	-	~ 0.81	0.88	8
Fe/Co-Nx doped porous carbon	0.72	0.89	-	5%	-	-	9
(FeSO4-PEI)LH	0.68	0.79	3.76 - 3.9	5-12%	0.736	0.84	10
Fe-P-C	-	0.84	3.8	4.13	~ 0.80	~ 0.89	11
Co-/Fe-coordinating pyrolyzed polymer	0.73	0.84	-	-	0.83	0.93	12
Fe-Co/NF-GNF	0.77	0.91	3.99	below 1%	0.83	093	13
CoFeNx/C	0.68	0.82	3.8	-	-	-	14
NFeCo-CNT/NC	0.75	0.84	3.95-4.0	below 3.2%	~ 0.82	0.91	15
Py-FCC/C-50	0.71	0.82	3.96	below 2.3%	0.75	0.88	This work

Table S5 A comparsion synthetic approaches of different metal-N/C catlysts for the preparation of various electrocatalysts for ORR

Material	Precursor	Carbon source	Heat treatment	Reaction condition	Etching process	Dispersion process	Ref.
$FeFe_2$-CNl 900/CA	Sucrose, FeCl3 $K_4Fe(CN)_6 \cdot 3H_2O$,	Sucrose, XC-72R nanpoartic le	Three step pyrolysis Step 1: 150 °C, 7 hours; Step 2: 300 °C, 2 hours; Step 3: 900 °C, 2 hours.	U/Vacuum	10 wt% HF	-	16
M1M2-CNl 600 (M1: Pt, Au, Ir, M2: Ir, Ni, Rh)	M-chlorides (M: At, Pt, Ir, Rh), M-cyanides (M: Pt, Ni)	Sucrose, XC-72R	Pyrolysis: 300 °C, 2 hours 600 °C, 2 hours	U/Vacuum	H_2O_2, (10 vol%)	Ball milling	17
PtNi-CNl 600/S500	$K_2Ni(CN)_4$, K_2PtCl_4, Sucrose,	Sucrose, XC-72R nanpoartic le	Step 1: 150 °C, 7 hours; Step 2: 300 °C, 2 hours; Step 3: 500/700 °C, 2 hours	U/Vacuum	H_2O_2 (5 vol.%)	Ball milling	18
Py-FCC/C-500	Ferrocene-Co-corrole	XC-72R	500 °C, 2 hours	U/N_2	-	Ball milling	This work

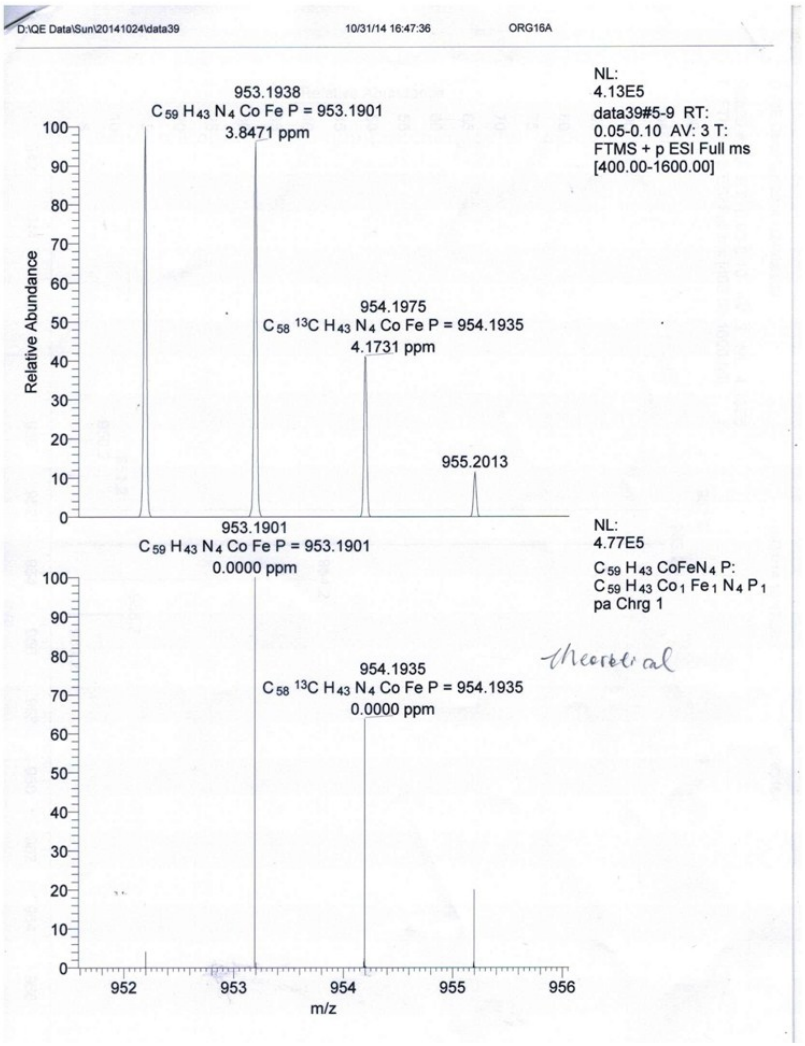

Fig. S13 HR-MS of FCC (observed: 953.1938, calculated: 953.1901).

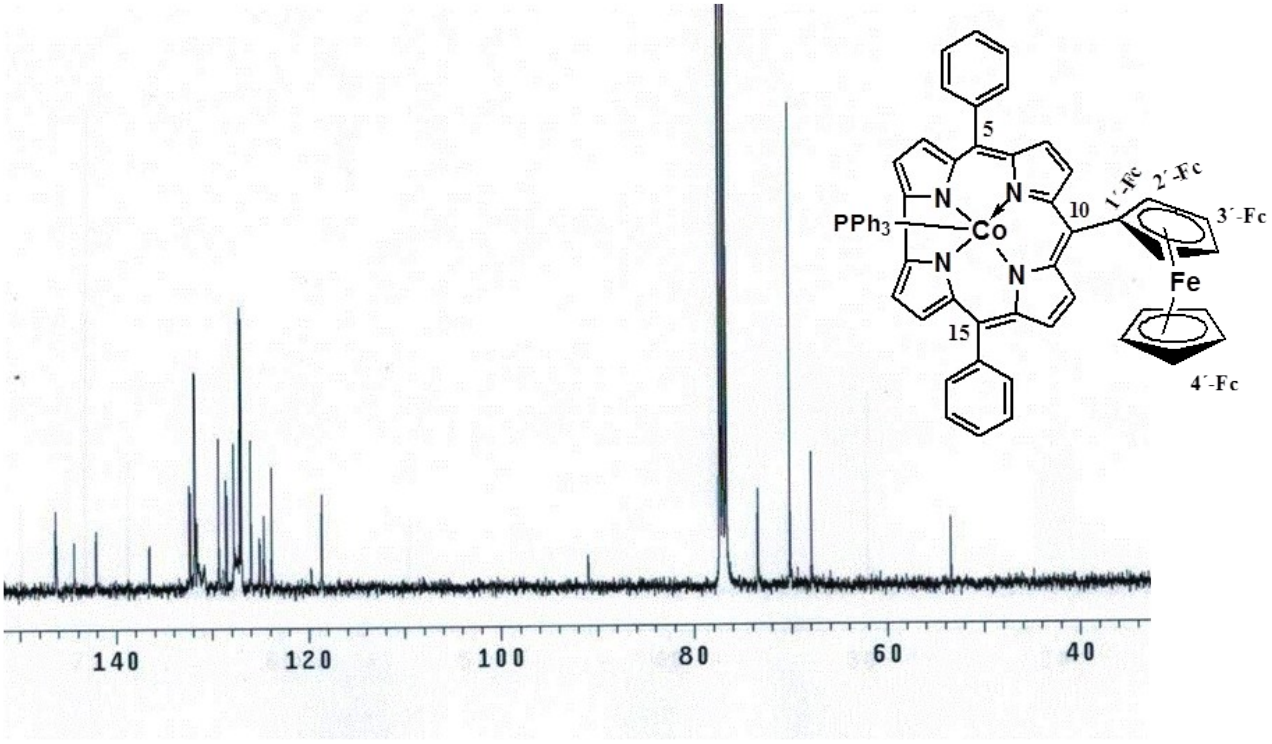

Fig. S14 ^{13}C NMR spectra of FCC.

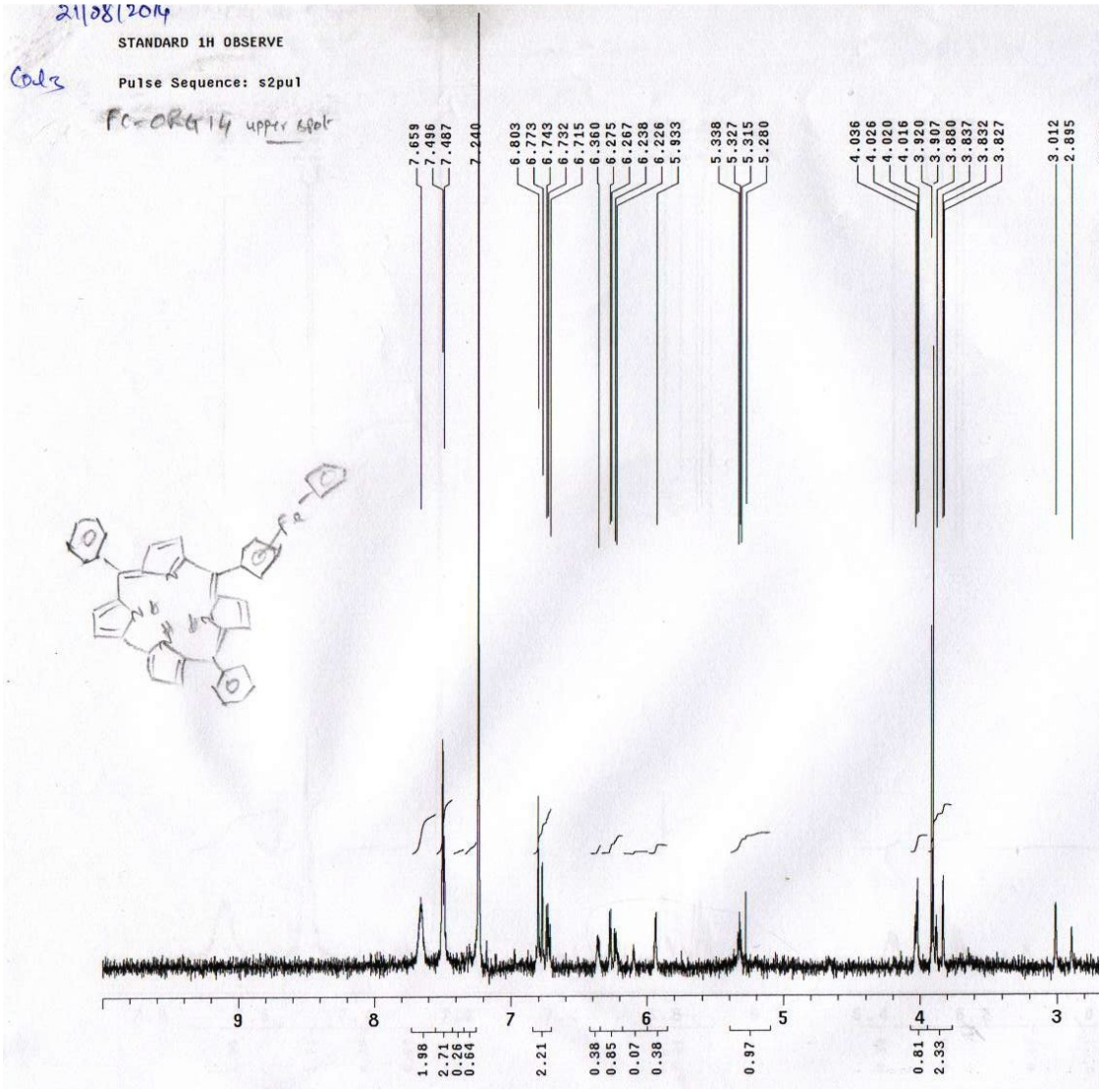

Fig. S15 ^{1}H NMR spectra of free-base corrole (1).

References

1. A. Spek, Journal of Applied Crystallography, 2003, **36**, 7.

2. H. E. Gottlieb, V. Kotlyar, A. Nudelman, J. Org. Chem., 1997, **62**, 7512.

3. J. N. Tiwari, K. Nath, S. Kumar, R. N. Tiwari, K. C. Kemp, N. H. Le, D. H. Youn, J. S. Lee, K. S. Kim, Nat. Commun., 2013, **4**, 2221.

4. S. Trasatti, O. A. Petrii, Pure Appl. Chem., 1991, **63**, 711.

5. H. Wang, Z. Lu, D. Kong, J. Sun, T. M. Hymel, Y. Cui, ACS Nano, 2014, **8**, 4940.

6. D. Malko, T. Lopes, E. Symianakis, A. R. Kucernak, J. Mater. Chem. A, 2016, **4**, 142.

7. S. Li, L. Zhang, J. Kim, M. Pan, Z. Shi, J. Zhang, Electrochim. Acta, 2010, **55**, 7346.

8. X. Wang, J. Zhou, H. Fu, W. Li, X. Fan, G. Xin, J. Zheng, X. Li, J. Mater. Chem. A, 2014, **2**, 14064.

9. J.-Y. Choi, R. S. Hsu and Z. Chen, J. Phys. Chem. C, 2010, **114**, 8048.

10. J. Shi, X. Zhou, P. Xu, J. Qiao, Z. Chen, Y. Liu, Electrochim. Acta, 2014, **145**, 259.

11. K. P. Singh, E. J. Bae, J.-S. Yu, J. Am. Chem. Soc., 2015, **137**, 3165.

12. Y. Zhao, K. Watanabe, K. Hashimoto, J. Am. Chem. Soc., 2012, **134**, 19528.

13. S. G. Peera, A. Arunchander, A. K. Sahu, Nanoscale, 2016, **8**, 14650.

14. R. Jiang, D. Chu, J. Power Sources, 2014, **245**, 352.

15. G. Wang, W.-hua Wang, Li.-K. Wang, W.-T. Yao, P.-F. Yao, W.-K. Zhu, P. Chen and Q.-S. Wu, J. Mater. Chem. A, 2015, **3**, 17866.

16. K. Vezzù, A. Bach Delpeuch, E. Negro, S. Polizzi, G. Nawn, F. Bertasi, G. Pagot, K. Artyushkova, P. Atanassov, V. Di Noto, Electrochim. Acta, 2016, **222**, 1778.

17. S. Diodati, E. Negro, K. Vezzù, V. Di Noto, S. Gross, Electrochim. Acta, 2016, **215**, 398.

18. V. Di Noto, E. Negro, S. Polizzi, K. Vezzù, L. Toniolo, G. Cavinato, Int. J. Hydrogen Energy, 2014, **39**, 2812.